Repeated eye reduction events reveal multiple pathways to degeneration in a family of marine snails

Article *in* Evolution · August 2016

DOI: 10.1111/evo.13022

5 authors, including:

Lauren Sumner-Rooney
Museum für Naturkunde - Leibniz Institute for …
8 PUBLICATIONS **25** CITATIONS
SEE PROFILE

Julia Sigwart
Queen's University Belfast
124 PUBLICATIONS **552** CITATIONS
SEE PROFILE

Lisa Smith
Natural History Museum, London
21 PUBLICATIONS **214** CITATIONS
SEE PROFILE

Suzanne T Williams
Natural History Museum, London
87 PUBLICATIONS **2,766** CITATIONS
SEE PROFILE

doi:10.1111/evo.13022

Repeated eye reduction events reveal multiple pathways to degeneration in a family of marine snails

Lauren Sumner-Rooney,[1,2,3] Julia D. Sigwart,[1,2] Jenny McAfee,[2] Lisa Smith,[4] and Suzanne T. Williams[5]

[1]School of Biological Sciences, Queen's University Belfast, Belfast BT9 7BL, Northern Ireland

[2]Queen's University Marine Laboratory, Queen's University Belfast, Portaferry, Co. Down BT22 1PF, Northern Ireland

[3]E-mail: lsumnerrooney01@qub.ac.uk

[4]Core Research Facility, Natural History Museum, Cromwell Road, London SW7 5BD, United Kingdom

[5]Department of Life Sciences, Natural History Museum, Cromwell Road, London SW7 5BD, United Kingdom

Received November 11, 2015

Accepted July 24, 2016

Eye reduction occurs in many troglobitic, fossorial, and deep-sea animals but there is no clear consensus on its evolutionary mechanism. Given the highly conserved and pleiotropic nature of many genes instrumental to eye development, degeneration might be expected to follow consistent evolutionary trajectories in closely related animals. We tested this in a comparative study of ocular anatomy in solariellid snails from deep and shallow marine habitats using morphological, histological, and tomographic techniques, contextualized phylogenetically. Of 67 species studied, 15 lack retinal pigmentation and at least seven have eyes enveloped by surrounding epithelium. Independent instances of reduction follow numerous different morphological trajectories. We estimate eye loss has evolved at least seven times within Solariellidae, in at least three different ways: characters such as pigmentation loss, obstruction of eye aperture, and "lens" degeneration can occur in any order. In one instance, two morphologically distinct reduction pathways appear within a single genus, *Bathymophila*. Even amongst closely related animals living at similar depths and presumably with similar selective pressures, the processes leading to eye loss have more evolutionary plasticity than previously realized. Although there is selective pressure driving eye reduction, it is clearly not morphologically or developmentally constrained as has been suggested by previous studies.

KEY WORDS: Deep sea, eye degeneration, eye loss, eye evolution, Solariellidae, vision, Vetigastropoda.

The reduction or loss of eyes is a common feature of animals that inhabit dark environments. This strong evolutionary pattern is found in vertebrates and invertebrates, in lifestyles that range from fossorial (e.g., Borghi et al. 2002) to cavernicolous (e.g., Sadoglu 1967) to abyssal (e.g., Hessler and Thistle 1975). The evolutionary mechanisms underlying eye loss have been the subject of debate since Darwin postulated that it could be attributed "wholly to disuse" (Darwin 1859; Rétaux and Casane 2013). In modern terms, this could be articulated as a release of stabilizing selective pressure on, and the subsequent accumulation of mutations in, genes involved in eye development and function (Fong et al. 1995). However, evolutionary experiments have since demonstrated that there is considerable directional selective pressure favoring eye loss in dark environments, for reasons of energetic economy or reinvestment in other sensory systems (Jones and Culver 1989; Yamamoto et al. 2004; Protas et al. 2007; Niven and Laughlin 2008). A particularly interesting emergent question is whether there is a common morphological mechanism or pattern to this process, or if it is driven randomly by neutral mutation or pleiotropy (Rétaux and Casane 2013). Eyes are likely to have evolved more than 40 times among animals and take many different forms (von Salvini-Plawen and Mayr 1977). Within most metazoan clades the basic structure of the eye is broadly conserved, such as vertebrate camera eyes, arthropod apposition or superposition compound eyes, and photosensitive light-spots in planarians. In addition, physical optical constraint

EVOLUTION INTERNATIONAL JOURNAL OF ORGANIC EVOLUTION

combined with evolutionary drive for high-quality vision has resulted in the convergent evolution of the camera eye in both vertebrates and cephalopods. A similarly convergent or restricted process led by morphological or developmental constraint might be expected where structurally similar eyes are lost.

Combined with a selective pressure in favor of eye loss, such evolutionary constraints could determine a most likely order of specific anatomical reduction events. Many authors have described groups of closely related organisms that have evolved convergent reduced or degenerate eye morphologies, characteristically including size reduction, loss of pigmentation, the envelopment of the eyes by the surrounding tissue, and degeneration of the optic nerve (Langecker and Longley 1993; Wilkens 2001; Wilkens and Strecker 2003; Protas et al. 2011). Although there is apparently selective pressure for eye loss, additional processes (drift, pleiotropy) are also doubtless implicated in its evolution: some authors have found evidence for a significant role played by the release of evolutionary constraint and subsequent neutral evolution in variety in the loss of eyes at both molecular and morphological levels (Niemiller et al. 2013). Thus, although there are common phenotypic changes that occur during eye reduction, some work has suggested that the specific order of their appearance is not predictable (Poulson 1963). But in other cases it appears that these characters evolve in the same way within groups, and as a result several authors have implied that the process of eye reduction is successive or predictable (Zharkova 1970; Brinton 1987; Wilkens 2001; Jäger 2012; Malkowsky and Götze 2014). This could have a developmental cause. Given the pleiotropic and highly conserved nature of many genes involved in vision and eye structure, certain loci may be targeted during eye reduction (e.g., Jeffery 2009). For example, the developmentally important *Hedgehog* appears to be repeatedly affected both within and between study systems (Leys et al. 2005; Protas et al. 2005; Aspiras et al. 2012). The majority of detailed work on the mechanisms of eye loss to date have used the cave fish *Astyanax mexicanus*, and further studies of eye reduction across a broader taxonomic range of dark-living species are needed to address this question (Malkowsky and Götze 2014). Several other cases of so-called regressive evolution have been similarly examined, such as limb loss in tetrapods and flight loss in ratites, which are both thought to have evolved independently in the same way multiple times (Lande 1978; Baker et al. 2014), but also the loss of the swim bladder in fishes, which has evolved in a more variable fashion (McCune and Carlson 2004). A macroscopic study of the morphological features of eye reduction across a relatively broad group of taxa has not been undertaken until now, and although some authors have acknowledged a need for such a study (e.g., Malkowsky and Götze 2014), none so far have addressed it directly.

Testing the extent to which eye reduction is a strictly constrained process requires a group of animals with relatively simple eye structure in which eye loss or reduction has evolved numerous times in closely related taxa, acting as a "natural experiment" (Harvey and Pagel 1991). Solariellidae is a family of small marine vetigastropods found worldwide from littoral to abyssal depths, and eye loss has been reported in several species across the family (Marshall 1999; Williams et al. 2013). This group provides an excellent opportunity to study the potential for anatomical determinism in eye loss and to draw comparisons among eyeless taxa, and offers a larger sample of eye reduction events than more commonly studied cavernicolous groups (Jeffery 2005; Tierney et al. 2015). Vetigastropods typically possess pigment cup eyes (Haszprunar 1988; Ponder and Lindberg 1997; Sasaki 1998; Kano and Kase 2002; Fig. 1). The retina consists of apically pigmented cells interspersed with rhabdomeric photoreceptors bearing microvilli and ciliary projections, and the basal side is surrounded by nerve tissue. The eye remains narrowly open, without a cornea, and a vitreous body fills the remainder of the cup and acts as a lens (Ponder and Lindberg 1997; Sasaki 1998). The phylogeny of the solariellids has been resolved by Williams et al. (2013), though here we expand upon that analysis with several new taxa. By comparing the microanatomy of solariellid eyes in a phylogenetic context we can infer the order of reductive elements and compare the anatomical pathways by which eye reduction occurs.

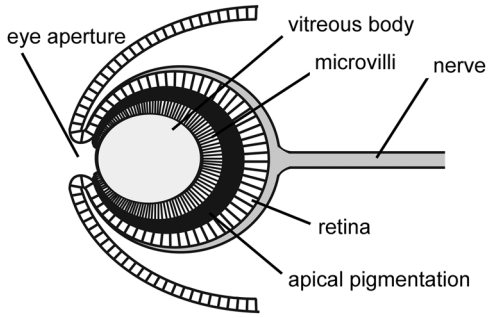

Figure 1. A typical solariellid eye (sagittal plane). The eye consists of an invaginated epithelial cup, which remains narrowly open, allowing light to enter. Rhabdomeric photoreceptors are surrounded by apically pigmented retinal cells and a central vitreous body acts as a lens.

Material and Methods

TAXON SELECTION

Sixty-seven species from across Solariellidae were selected for examination of gross eye morphology on the basis of depth, locality, and taxonomic position to cover a broad range in these fields. These represented 12 of the 14 accepted genera in Solariellidae, as well as one additional undescribed genus, and 67 of an estimated 250 species in the family. One of the nonincluded genera, *Lamellitrochus*, is likely to be a synonym of *Zetela*, which

was represented herein by four other species (Williams et al. 2013). Nine species, including three lacking pigmented eyes, were then selected for histological study to examine the nature and extent of eye reduction, if present. Specimens used for histological study were selected for their tissue quality, as well as to give a good taxonomic and ecological range. A number of undescribed species within the group are noted with the genus name and a numeral following the identifications of Williams et al. (2013). Since Williams et al. (2013) Clades A and C have been formally described as the genera *Arxellia* and *Elaphriella*, respectively, and several new species described (Vilvens et al. 2014; Vilvens and Williams 2016). We use the new names in this study. The shallow water species *Ilanga* 6 was included to give a model for comparison to the eyes of several deep-water species: *Elaphriella khantaros, Elaphriella wareni, Bathymophila diadema*, "*Bathymophila*" 18, *Zetela* 1, and *Zetela alphonsi*. We also included two species from intermediate depths, *Ilanga* 10 and *Spectamen mutabilis* (Williams et al. 2013). These were all found to belong to well-resolved clades by Williams et al. (2013), excepting "*Bathymophila*" 18 and *Z. alphonsi*, which were not included in that study. Preservation of *Z. alphonsi* precluded its inclusion in molecular analyses.

LABORATORY METHODS, SEQUENCE EDITING, AND ALIGNMENT

We followed the protocols of Williams et al. (2013) to extract DNA and amplify and sequence portions of the nuclear 28S rRNA gene (28S) and three mitochondrial genes: cytochrome oxidase subunit I (COI), 16S rRNA (16S), and 12S rRNA (12S). A total of 123 new sequences were added to a subset of previously published sequences for solariellids and five outgroup taxa from appropriate vetigastropod clades (three in Calliostomatidae and two Trochidae) from Williams (2012) and Williams et al. (2013) (new EMBL accession numbers in Table 1, SD6).

Alignments were made in Geneious (v.6.1.7, Kearse et al. 2012), starting with Geneious own alignment and then refined using default settings in Muscle (Edgar 2004) and ClustalW (Larkin et al. 2002) plugins within Geneious. Poorly aligned sites in rRNA alignments were identified using Gblocks Server (0.91b, Castresana 2000) and excluded from analyses. Parameters used in Gblocks allowed for smaller final blocks, gap positions within the final blocks and less strict flanking positions.

PHYLOGENETIC AND ANCESTRAL STATE RECONSTRUCTION

Bayesian phylogenies were determined using MrBayes (v.3.2.2, Huelsenbeck and Ronquist 2001) following the protocol used in Williams et al. (2013) and run on the CIPRES portal (Miller et al. 2010). The best nucleotide substitution models were determined to be GTR+G for 28S and 16S and HKY+I+G for COI and 12S using Akaike Information Criterion (AIC) calculated with jModelTest (Guindon and Gascuel 2003; Darriba et al. 2012). Analyses were run for 20,000,000 generations with a sample frequency of 1000 in two independent runs. The first ten percent were discarded, so that the final tree was computed from a total of 36,000 trees. Stationarity and convergence between the two runs were determined by examining the potential scale reduction factors (PSRF), standard deviation of split frequencies and by visual examination of .p files in Tracer (v. 1.5; available from http://beast.bio.ed.ac.uk/Tracer).

A combined gene tree was produced in MrBayes including up to three specimens per species for species in the tree published in Williams et al. (2013), plus all available specimens for new taxa, where specimens have sequences for 28S plus at least two mitochondrial genes. Exceptions to this rule were made for three individuals missing data, as they were the only representatives of their species: *Solariella affinis* (NHMUK 20120233), *Solariella* 6 (MNHN IM-2007-18537), and *Bathymophila* 21 (MNHN IM-2009-15206). Single gene trees for 12S and COI were also produced to confirm species identifications for some specimens not included in the combined gene tree.

We used BEAST (v.1.8.3; Drummond et al. 2012) to analyze molecular data incorporating fossil calibrations. We used the combined gene dataset, but pruned replicate taxa, so that each species was represented by a single specimen sequence. We unlinked all clocks and substitution rates, but linked trees for all four genes. Three monophyletic taxon sets were defined: ingroup (starting age 75 Ma), *Solariella* (starting age 25 Ma) and *Zetela* (starting age 20 Ma), and analyses were performed without including any outgroup sequences. These groups follow the same constraints and fossil calibrations used in Williams et al. (2013). The ingroup was constrained to be at least 71 Ma (95% interval: 71.4–89 Ma; mean in real space: 4.18, log stdev: 1, offset: 71). The *Solariella* clade was constrained to be at least 23 Ma (95% interval: 23.2–34 Ma; mean in real space: 2.555, log stdev: 1, offset: 23). The *Zetela* clade was constrained to be at least 16.7 Ma (95% interval: 16.7–27.9 Ma; mean in real space: 2.65, log stdev: 1, offset: 16.5) (see Williams et al. 2013 for justification of fossil choices). Nucleotide substitution models were those chosen by jModelTest, except the model for 16S that was simplified to HKY+G after preliminary runs. Uncorrelated relaxed, lognormal clocks were used for all genes, with a birth-death speciation prior and a random starting tree. We used a diffuse gamma distribution (shape 0.001, scale 1000) for the ucld.mean parameters. The analysis ran for 100,000,000 generations with trees sampled every 10,000 steps.

Additional supporting phylogenetic analyses under parsimony were run in POY (Varón et al. 2010) using the same sequence data. Analyses used incongruent length difference parameter set 141 (with a simulated cost ratio of indel/

Table 1. Catalog data of all specimens examined, with GenBank accession numbers for sequence data used in phylogenetic analyses.

Species	Reg	Locality	Lat/Long	Depth (m)	Expedition/ Station	P	A	28S	COI	16S	12S
Archiminolia 1	MNHN IM-2007-18540	S. Gatukai Island	9°06.9' S, 158° 21' E	267–329	Solomon 2/ DW2301	Y	Y	HF586167	HF586310	HF586019	HF585858
Archiminolia 2	MNHN IM-2007–18316	N Bellona, New Caledonia	20° 23 S, 158° 45' E	324–330	EBISCO/ CP2572	Y	Y	HF586168	HF586311	HF586020	HF585859
Archiminolia 2	MNHN IM-2007–18339	Norfolk Ridge, Banc Kaimon Maru	23° 24' S, 168° 00' E	400	NORFOLK2/ DW2117	Y	Y	–	–	–	HF585862
Archiminolia 2	MNHN IM-2009–8804	Norfolk Ridge, Banc Antigonia	23° 23' S, 168° 00' E	430–480	TERRASSES/ DW3063	Y	Y	HF586172	HF586315	HF586024	HF585864
Archiminolia 2	MNHN IM-2009–8867	Norfolk Ridge, Munida	23° 01' S, 168° 23' E	380–440	TERRASSES/ DW3107	Y	Y	HF586173	HF586316	HF586025	HF585865
Archiminolia 2	MNHN IM-2009–15176	Norfolk Ridge, Munida	23° 01' S, 168° 23' E	380–440	TERRASSES/ DW3107	Y	Y	–	LT575866	–	–
Archiminolia 3	MNHN IM-2013–19973	E Umboi I., Dampier Strait, Papua New Guinea	05°40'S 148°14'E	208–285	PAPUA NIUGUINI/ CP4016	Y	Y	LT575948	LT575867	LT575905	LT575924
Archiminolia 3	MNHN IM-2013–19974	E Umboi I., Dampier Strait, Papua New Guinea	05°40'S 148°14'E	208–285	PAPUA NIUGUINI/ CP4016	Y	Y	LT575949	LT575868	LT575903	LT575922
Archiminolia 3	MNHN IM-2013–19975	E Umboi I., Dampier Strait, Papua New Guinea	05°40'S 148°14'E	208–285	PAPUA NIUGUINI/ CP4016	Y	Y	LT575950	LT575869	LT575904	LT575923
Archiminolia oleacea	AM C133269.001	N of Fraser I., Queensland, Australia	24.375°S, 153.285°	192–229	HMAS Kimbla/25	N	?	–	–	–	–
Archiminolia oleacea	AM C133269.001	N of Fraser I., Queensland, Australia	24.375°S, 153.285°	192–229	HMAS Kimbla/25	N	?	–	–	–	–

(*Continued*)

Table 1. Continued.

Species	Reg	Locality	Lat/Long	Depth (m)	Expedition/ Station	P	A	28S	COI	16S	12S
Archiminolia oleacea	AM C133269.001	N of Fraser I., Queensland, Australia	24.375°S, 153.285°	192–229	HMAS Kimbla/25	N	?	–	–	–	–
Archiminolia oleacea	AM C133269.001	N of Fraser I., Queensland, Australia	24.375°S, 153.285°	192–229	HMAS Kimbla/25	N	?	–	–	–	–
Archiminolia oleacea	AM C133269.001	N of Fraser I., Queensland, Australia	24.375°S, 153.285°	192–229	HMAS Kimbla/25	N	?	–	–	–	–
Arxellia helicoides	NHMUK 20140009	Seamount S of Manus I., Papua New Guinea	3°04'S, 147°32'E	402–640	DW3688	Y	Y	HF586157	HF586300	–	HF585846
Arxellia tenorioi	MNHN IM-2007–18429	Bohol Sea, off Balicasag Island, Philippines	9°28.6'N, 123° 40.0'E	470–566	PANGLAO2005	Y	Y	HF586165	HF586308	HF586017	HF585856
Arxellia tenorioi	MNHN IM-2007–18394	Bohol Sea, off Balicasag Island, Philippines	9°31.7'N, 123°41.9'E	309–342	PANGLAO2005	Y	Y	HF586166	HF586309	HF586018	HF585843
Arxellia cf. thaumasta	WAM S25779	off Point Hillier, Western Australia	35.3818°S, 117.2030°I	419–460	SS1005/020	Y	Y	–	–	–	–
Arxellia tracheia	MNHN IM-2013–19897	SE Tuam I., Papua New Guinea	06°03'S 148°08'E	440	PAPUA NIUGUINI/ DW4004	Y	Y	–	LT596067	–	–
Arxellia tracheia	MNHN IM-2013–19898	SE Tuam I., Papua New Guinea	06°03'S 148°08'E	440	PAPUA NIUGUINI/ DW4004	Y	Y	–	LT596068	–	–
Arxellia tracheia	MNHN IM-2013–19899	SE Tuam I., Papua New Guinea	06°03'S 148°08'E	440	PAPUA NIUGUINI/ DW4004	Y	Y	–	LT596069	–	–
Arxellia tracheia	MNHN IM-2013–19901	SE Tuam I., Papua New Guinea	06°04'S 148°08'E	440–480	PAPUA NIUGUINI/ DW4005	Y	Y	–	LT596070	–	–

(*Continued*)

Table 1. Continued.

Species	Reg	Locality	Lat/Long	Depth (m)	Expedition/ Station	P	A	28S	COI	16S	12S
Arxellia trochos	MNHN IM-2009–23089	Banc de L'Orne/ Walpole, New Caledonia	22°20'S, 169°01'E	400–520	EXBODI/ DW3862	Y	–	LT596065	LT596072	LT596062	LT596058
Arxellia trochos	MNHN IM-2009–23092	Banc de L'Orne/ Walpole, New Caledonia	22°20'S, 169°01'E	400–520	EXBODI/ DW3862	Y	Y	LT596066	LT596073	LT596063	LT596059
Arxellia trochos	MNHN IM-2009–23094	Banc de L'Orne/ Walpole, New Caledonia	22°19'S, 169°01'E	425–490	EXBODI/ DW3861	–	–	–	LT575870	–	LT575925
Arxellia trochos	MNHN IM-2009–23109	Banc Sud Durand, New Caledonia	22°19'S, 168°45'E	471–510	EXBODI/ CP3851	Y	Y	LT575951	LT575871	LT575906	LT575926
Arxellia trochos	NHMUK 20140006	Banc de L'Orne/ Walpole, New Caledonia	22°20'S, 169°01'E	400–520	EXBODI/ DW3862	Y	Y	LT596064	LT596071	LT596061	LT596057
Bathymophila diadema	MNHN IM-2007–18311	W Bellona, New Caledonia	21° 06' S, 158° 32' E	741–791	EBISCO/ CP2556	Y	N	HF586079	HF586219	HF585929	HF585753
Bathymophila diadema	**MNHN IM-2007–18319**	**SE Fairway, New Caledonia**	**21° 29' S, 162° 36' E**	**883–957**	**EBISCO/ CP2651**	Y	N	**HF586081**	**HF586221**	**HF585931**	**HF585755**
Bathymophila diadema	MNHN IM-2007–18320	SE Fairway, New Caledonia	21° 29' S, 162° 36' E	883–957	EBISCO/ CP2651	Y	N	HF586082	HF586222	HF585932	HF585756
Bathymophila diadema	MNHN IM-2007–18535	NW Vella, Lavella I., Solomon Islands	7° 31.3' S, 156° 17.7' E	782–884	SALOMON2/ CP2249	Y	N	–	HF586223	–	HF585725
Bathymophila diadema	MNHN IM-2009–8869	Loyalty Ridge	23° 48' S, 169° 46' E	660–710	TERRASSES/ DW3045	Y	N	HF586084	HF586226	HF585934	HF585761
Bathymophila diadema	MNHN IM-2009–8871	Loyalty Ridge	23° 48' S, 169° 46' E	660–710	TERRASSES/ DW3045	Y	N	HF586085	HF586227	HF585935	HF585762

(*Continued*)

Table 1. Continued.

Species	Reg	Locality	Lat/Long	Depth (m)	Expedition/ Station	P	A	28S	COI	16S	12S
Bathymophila diadema	MNHN IM-2009–13010	NW Vella, Lavella I., Solomon Islands	7° 31.3' S, 156° 17.7' E	782–884	SALOMON2/ CP2249	Y	N	–	–	–	HF585757
Bathymophila diadema	MNHN IM-2009–13011	NW Vella, Lavella I., Solomon Islands	7° 31.3' S, 156° 17.7' E	782–884	SALOMON2/ CP2249	Y	N	–	HF586224	–	HF585758
Bathymophila diadema	MNHN IM-2009–13012	NW Vella, Lavella I., Solomon Islands	7° 31.3' S, 156° 17.7' E	782–885	SALOMON2/ CP2249	Y	N	–	–	–	–
Bathymophila diadema	MNHN IM-2009–15191	Off Bougainville, Papua New Guinea	5° 04' S, 154° 29' E	662	BIOPAPUA/ CP3755	Y	N	HF586088	HF586229	HF585938	HF585764
Bathymophila diadema	MNHN IM-2009–15198	Off Bougainville, Papua New Guinea	05°02'S, 154°29'E	615–632	BIOPAPUA/ DW3754	Y	N	–	LT575872	–	–
Bathymophila diadema	MNHN IM-2009–15199	Off Bougainville, Papua New Guinea	05°02'S, 154°29'E	615–632	BIOPAPUA/ DW3754	Y	N	–	LT575873	–	–
Bathymophila diadema	MNHN IM-2009–15200	Off Bougainville, Papua New Guinea	05°02'S, 154°29'E	615–632	BIOPAPUA/ DW3754	Y	N	–	LT575874	–	–
Bathymophila diadema	MNHN IM-2009–15217	Off Bougainville, Papua New Guinea	05°04'S, 154°29'E	662	BIOPAPUA/ CP3755	Y	N	–	–	–	LT596060
Bathymophila diadema	MNHN IM-2009–15221	Off Bougainville, Papua New Guinea	05°04'S, 154°29'E	662	BIOPAPUA/ CP3755	Y	N	–	–	–	–

(*Continued*)

Table 1. Continued.

Species	Reg	Locality	Lat/Long	Depth (m)	Expedition/ Station	P	A	28S	COI	16S	12S
Bathymophila sp 2	MNHN IM-2007–18323	Chesterfield, New Caledonia	19° 38' S, 158° 44' E	569–570	EBISCO/ DW2584	Y	N	HE800722	HE800623	HE800762	HE800673
Bathymophila sp 4	MNHN IM-2009–8762	Between Nosy-bé and Banc du Leven, Madagascar	12° 47' S, 48° 08' E	784	MIRIKY/ CP3221	Y	N	HF586089	HF586230	HF585939	HF585765
Bathymophila sp 4	MNHN IM-2009–8764	Between Nosy-bé and Banc du Leven, Madagascar	12° 47' S, 48° 08' E	783	MIRIKY/ CP3221	Y	N	HF586091	HF586232	–	HF585767
Bathymophila sp 4	MNHN IM-2009–8769	Between Nosy-bé and Banc du Leven, Madagascar	12° 26' S, 48° 13'E,	578–782	MIRIKY/ CP3192	Y	N	HF586092	HF586233	HF585941	HF585768
Bathymophila sp 4	MNHN IM-2009–8770	Between Nosy-bé and Banc du Leven, Madagascar	12° 34' S, 48° 09' E	613–625	MIRIKY/ CP3186	Y	N	HF586093	HF586234	HF585942	HF585769
Bathymophila sp 4	MNHN IM-2009–8772	Between Nosy-bé and Banc du Leven, Madagascar	12° 47' S, 48° 08' E	782	MIRIKY/ CP3221	Y	N	HF586095	HF586236	HF585944	HF585771
Bathymophila sp 4	MNHN IM–2009–8773	Between Nosy-bé and Banc du Leven, Madagascar	12° 47' S, 48° 08' E	782	MIRIKY/ CP3221	Y	N	HF586096	HF586237	HF585945	HF585772
Bathymophila sp 6	MNHN IM-2007–35547	Grand Passage, New Caledonia	17°59'S, 163°03'E	650–700	CONCALIS	N	?	HF586097	HF586238	HF585946	HF585773
Bathymophila sp 7	MNHN IM-2007–18317	SE Fairway, New Caledonia	21°29'S, 162°36'E	883–957	EBISCO/ CP2651	N	?	HF586098	HF586239	HF585947	HF585774

(*Continued*)

Table 1. Continued.

Species	Reg	Locality	Lat/Long	Depth (m)	Expedition/ Station	P	A	28S	COI	16S	12S
Bathymophila n.s. 7	MNHN IM-2009–23095	Ile Matthew-Volcan, New Caledonia	22°19'S, 171°20'E	925	EXBODI/ DW3879	N	?	LT575952	LT575876	LT575907	LT575927
Bathymophila sp 9	MNHN IM-2007–35590	Grand Passage, New Caledonia	19°00'S, 163°26' E	285–300	CONCALIS/ DW3023	N	?	HF586100	HF586241	HF585949	HF585779
Bathymophila sp 10	MNHN IM-2009–15182	Vitiaz Straight, Papua New Guinea	05°59'S, 147°39'E	860–880	BIOPAPUA/ CP3724?	N	?	HF586101	HF586242	HF585950	HF585781
Bathymophila sp 11	MNHN IM-2009–15175	Niau, Tuamotu Archipelago	16°08'S, 146°24'W	412–520	TARASOL/ DW3369	N	?	HF586102	HF586243	HF585951	HF585787
Bathymophila sp 15	YK1383	SW of Nagasaki, Japan	32°10'N, 129°30'E	470–487	T/V Nagasaki-Maru N226	N	?	HF586103	HF586244	HF585952	HF585782
Bathymophila sp 16	YK1385	Between Ambrim and Malekula, Vanuatu	16°19'S, 167°47'E	657–685	BOA1	N	?	HF586104	–	HF585953	HF585783
***Bathymophila n.s.* 18**	**MNHN IM-2009–23080**	**Ile Matthew-Volcan, New Caledonia**	**22°19'S, 171°20'E**	**925**	**EXBODI/ DW3879**	**N**	**Y**	LT575953	LT575877	LT575908	LT575929
Bathymophila n.s. 18	MNHN IM-2009–23100	Ile Matthew-Volcan, New Caledonia	22°19'S, 171°20'E	925	EXBODI/ DW3879	N	?	LT575954	LT575880	LT575909	LT575930
Bathymophila n.s. 18	MNHN IM-2009–23101	Ile Matthew-Volcan, New Caledonia	22°19'S, 171°20'E	925	EXBODI/ DW3879	N	?	LT575955	LT575879	LT575912	LT575931
Bathymophila n.s. 18	MNHN IM-2009–23103	Ile Matthew-Volcan, New Caledonia	22°19'S, 171°20'E	925	EXBODI/ DW3879	N	?	LT575957	–	LT575910	LT575928
Bathymophila n.s. 18	MNHN IM-2009–23104	Ile Matthew-Volcan, New Caledonia	22°19'S, 171°20'E	925	EXBODI/ DW3879	N	?	LT575956	LT575878	LT575911	LT575932
Bathymophila n.s. 19	MNHN IM-2009–23081	N Ile Matthew-Volcan, New Caledonia	22°17'S, 171°18'E	785	EXBODI/ DW3877	N	?	LT575960	–	LT575914	LT575935

(*Continued*)

Table 1. Continued.

Species	Reg	Locality	Lat/Long	Depth (m)	Expedition/ Station	P	A	28S	COI	16S	12S
Bathymophila n.s. 20	MNHN IM-2009–23082	Ile Matthew-Volcan, New Caledonia	22°19'S, 171°20'E	925	EXBODI/ DW3879	N	?	LT575958	LT575881	–	LT575933
Bathymophila n.s. 20	MNHN IM-2009–23102	Ile Matthew-Volcan, New Caledonia	22°19'S, 171°20'E	925	EXBODI/ DW3879	N	?	LT575959	LT575882	LT575913	LT575934
Bathymophila sp 21	MNHN IM-2009–15206	Seamounts near Bougainville, Papua New Guinea	05°33'S, 153°59'E	458	BIOPAPUA/ CP3747	Y	Y	–	LT575875	–	–
Clade B sp 2	MNHN IM-2009–8739	Mozambique Channel	23° 33' S, 36° 02' E	886–898	MAINBAZA/ CP3140	Y	Y	HE800720	HE800621	HE800760	HE800671
Clade B sp 2	MNHN IM-2009–8742	Maputo transect, Mozambique Channel	23° 33' S, 36° 02' E	886–898	MAINBAZA/ CP3140	Y	Y	HF586070	HF586211	HF585920	HF585744
Clade B sp 3	YK1407	SW of Nagasaki, Japan	32°09'N, 129°31'E	498–503	T/V Nagasaki-Maru N295	Y	Y	HF586072	HF586213	HF585922	HF585746
Elaphriella helios	MNHN IM-2007–18426	Bohol Sea, off Balicasag Island, Philippines	9°32.6'N, 123° 40.5'E	713–731	PANGLAO2005	Y	Y	HF586060	HF586206	HF585910	HF585732
Elaphriella khantaros	MNHN IM-2009–15201	Near Bougainville, Papua New Guinea	05°04'S, 154°29'E	662	BIOPAPUA/ CP3755	Y	N	–	LT575883	–	–
Elaphriella khantaros	MNHN IM-2009–15214	Off Bougainville, Papua New Guinea	05°02'S, 154°29'E	615–632	BIOPAPUA/ CP3754	Y	N	–	–	–	LT575936
Elaphriella khantaros	MNHN IM-2009–15218	Off Bougainville, Papua New Guinea	05°04'S, 154°29'E	662	BIOPAPUA/ CP3755	Y	N	–	–	–	–

(*Continued*)

Table 1. Continued.

Species	Reg	Locality	Lat/Long	Depth (m)	Expedition/ Station	P	A	28S	COI	16S	12S
Elaphriella khantaros	MNHN IM-2009–15220	W of New Hanover, Papua New Guinea	02°13'S, 150°23'E	680–700	BIOPAPUA/ CP3653	Y	N	–	–	–	LT575937
Elaphriella khantaros	MNHN IM-2009–15235	W of New Hanover, Papua New Guinea	02°13'S, 150°23'E	680–700	BIOPAPUA/ CP3653	Y	N	–	–	–	–
Elaphriella khantaros	MNHN IM-2009–15236	W of New Hanover, Papua New Guinea	02°13'S, 150°23'E	680–700	BIOPAPUA/ CP3653	Y	N	–	–	–	–
Elaphriella khantaros	MNHN IM-2009–33821	Off Bougainville, Papua New Guinea	05°02'S, 154°29'E	615–632	BIOPAPUA/ DW3754	Y	N	–	–	–	–
Elaphriella khantaros	**MNHN IM-2009–43073**	**W. Vella, Solomon Islands**	**7°42.9'S, 156°27.3'E**	**518–527**	**SALOMON2/ CP2243**	**Y**	**N**	**HF586063**	**HF586208**	**HF585913**	**HF585736**
Elaphriella n.s. 1	YK13847	SW of Nagasaki, Kyushu Island	32°10'N, 129°30'E	470-487	T/V Nagasaki–Maru, N226	Y	Y	HF586069	HF586210	HF585919	HF585743
Elaphriella n.s. 2	MNHN IM-2013–19896	SE Tuam I., Papua New Guinea	06°03'S, 148°08'E	440	PAPUA NIUGUINI/ DW4004	Y	Y	LT575961	LT575884	LT575915	LT575938
Elaphriella paulinae	MNHN IM-2009–23099	Banc Sud Durand, New Caledonia	22°18'S, 168°46'E	692	EXBODI/ CP3853	Y	N	–	LT575885	–	–
Elaphriella wareni	**MNHN IM-2009–18318**	**SE Fairway, New Caledonia**	**21°29'S, 162°36'E**	**883–957**	**EBISCO/ CP2651**	**N**	**N**	**HF586058**	**–**	**HF585908**	**HF585729**

(*Continued*)

Table 1. Continued.

Species	Reg	Locality	Lat/Long	Depth (m)	Expedition/ Station	P	A	28S	COI	16S	12S
Hazuregyra watanabei	YK1464	Off Kinkazan, Miyagi, Honshu Island, Japan	37°59'N, 141°59'E	350	R/V Wakataka-maru	Y	Y	HF586105	HF586245	HF585954	HF585784
Ilanga 1	MNHN IM-2009–15207	Seamounts near Bougainville, Papua New Guinea	05°37'S, 154°01'E	398–399	BIOPAPUA/ DW3748	Y	Y	–	LT575886	–	–
Ilanga 1	MNHN IM-2009–15208	Seamounts near Bougainville, Papua New Guinea	05°37'S, 154°01'E	398–399	BIOPAPUA/ DW3748	Y	Y	–	LT575888	–	–
Ilanga 1	MNHN IM-2009–15209	Seamounts near Bougainville, Papua New Guinea	05°37'S, 154°01'E	398–399	BIOPAPUA/ DW3748	Y	Y	–	LT575887	–	–
Ilanga 1	MNHN IM-2009–15237	Seamounts near Bougainville, Papua New Guinea	05°37'S, 154°01'E	398–399	BIOPAPUA/ DW3748	Y	Y	–	LT575889	–	–
Ilanga 3	MNHN IM-2007–18301	Malo Island, Vanuatu	15°42'S, 167°02'E	268–445	BOA1	Y	Y	HF586114	HF586253	HF585964	HF585796
Ilanga 4	MNHN IM-2007–18548	Off Tashi, Taiwan	24°57'N, 122°02'E	115–170	TAIWAN2001	Y	Y	–	–	–	HF585803
***Ilanga* 6**	**MNHN IM-2009–31831**	**E Aoré Island, off Aimbuei Bay, Vanuatu**	**15°34.9'S, 167°13.9'E**	**10–51**	**SANTO2006/ EP35**	Y	Y	**–**	LT575890	**–**	**–**
Ilanga 9	MNHN IM-2007–18315	N. Bellona, New Caledonia	20°25'S, 158°45'E	298–309	EBISCO	Y	Y	HF586138	HF586279	HF585988	HF585823
Ilanga 9	MNHN IM-2007–18326	Lansdowne, New Caledonia	20°06'S, 160°23'E	280–304	EBISCO	Y	Y	HF586139	HF586280	HF585989	HF585824
Ilanga 10	MNHN IM-2009–8797	SE Terrasses, New Caledonia	22°13'S, 167°12'E	360–380	TERRASSES/ CP3092	Y	Y	–	–	–	HF585828

(*Continued*)

Table 1. Continued.

Species	Reg	Locality	Lat/Long	Depth (m)	Expedition/ Station	P	A	28S	COI	16S	12S
Ilanga 10	MNHN IM-2009–15222	SE Terrasses, New Caledonia	22.19°S, 167.16°E	360–380	TERRASSES/ CP3092	Y	Y	–	LT575891	–	–
Ilanga 10	MNHN IM-2009–15223	SE Terrasses, New Caledonia	22.19°S, 167.16°E	360–380	TERRASSES/ CP3092	Y	Y	–	LT575892	–	–
Ilanga 10	MNHN IM-2009–15224	SE Terrasses, New Caledonia	22.19°S, 167.16°E	360–380	TERRASSES/ CP3092	Y	Y	–	LT575893	–	–
Ilanga 10	MNHN IM-2009–15225	SE Terrasses, New Caledonia	22.19°S, 167.16°E	360–380	TERRASSES/ CP3092	Y	Y	–	LT575894	–	–
Ilanga 10	MNHN IM-2009–15226	SE Terrasses, New Caledonia	22.19°S, 167.16°E	360–380	TERRASSES/ CP3092	Y	Y	–	LT575895	–	–
***Ilanga* 10**	**MNHN IM-2009–23091**	**Off Yaté, New Caledonia**	**22°06'S, 167°06'E**	**325–346**	**EXBODI/ CP3833**	Y	Y	**–**	LT575896	**–**	LT575939
Ilanga 10	MNHN IM-2009–23098	Off Yaté, New Caledonia	22°02'S 167°04'E	325–332	EXBODI/ CP3833	Y	Y	–	–	–	LT575940
Ilanga 10	MNHN IM-2009–43071	Canal de la Havannah, New Caledonia	22°14'S, 167°11'E	378–414	EXBODI/ CP3790	Y	Y	–	–	–	LT575940
Ilanga 11	MNHN IM-2009–15174	Maputo transect, Mozambique	23°32'S, 35°46'E	264–277	MAINBAZA	Y	Y	HF586106	–	HF585956	HF585890
Ilanga 12	MNHN IM-2009–13003	Between Panglao and Pamilacan Island, Philippines	9°33.4'N, 123°51.0'E	106–137	PANGLAO2004	Y	Y	HF586126	HF586267	HF585977	HF585810
Ilanga 15	MNHN IM-2009–15196	Off Feni Island, Papua New Guinea	04°00'S, 153°36'E	287–352	BIOPAPUA	Y	Y	HF586113	HF586252	HF585963	HF585795

(*Continued*)

Table 1. Continued.

Species	Reg	Locality	Lat/Long	Depth (m)	Expedition/ Station	P	A	28S	COI	16S	12S
Ilanga 16	MNHN IM-2009–8801	SE Terrasses, New Caledonia	22°04'S, 167°03'E	250–300	TERRASSES	Y	Y	HF586121	HF586262	HF585972	HF585805
Ilanga 17	MNHN IM-2007–18416	Bohol Sea, Maribojoc Bay Philippines	9°38.2'N, 123° 43.5'E	584–596	PANGLAO2005	Y	Y	HF586115	HF586254	HF585965	HF585797
Ilanga 17	MNHN IM-2007–18417	Bohol Sea, Maribojoc Bay Philippines	9°39.2'N, 123°47.5'E	255–268	PANGLAO2005	Y	Y	HF586116	HF586255	HF585966	HF585798
Ilanga n.s. 21	WAM S84074	Off Red Bluff, Western Australia	24° 1.03'S, 113° 2.03'E	100-101	Southern Surveyor/ SS1005/133	Y	Y	LT575962	LT575897	LT575916	LT575942
Ilanga biradulata	MNHN IM-2009–8740	Maputo transect, Mozambique	25°13'S, 35°18'E	480–503 m	MAINBAZA	Y	Y	HE800723	HE800624	HE800763	HE800674
Ilanga biradulata	MNHN IM-2009–8741	Maputo transect, Mozambique	25°13'S, 35°18'E	480–503 m	MAINBAZA	Y	Y	HF586133	HF586274	HF585984	HF585818
Ilanga discus	MNHN IM-2009–8758	Between Nosy-bé and Banc du Leven, Madagascar	12° 31' S, 48° 22' E	298–301	MIRIKY	Y	Y	HF586109	HF586248	HF585959	HF585791
Ilanga discus	MNHN IM-2009–8760	Between Nosy-bé and Banc du Leven, Madagascar	12° 31' S, 48° 22' E	298–301	MIRIKY	Y	Y	HF586110	HF586249	HF585960	HF585792

(*Continued*)

Table 1. Continued.

Species	Reg	Locality	Lat/Long	Depth (m)	Expedition/ Station	P	A	28S	COI	16S	12S
Ilanga discus	MNHN IM-2009–8761	Between Nosy-bé and Banc du Leven, Madagascar	12° 31' S, 48° 22' E	298–301	MIRIKY	Y	Y	HE800724	HE800625	HE800764	HE800675
Ilanga laevissima	NMSA V4397	Plettenberg Bay, South Africa	34°19.5'S, 23°30'E	104	NMDP (Africana)	Y	Y	HF586151	HF586293	HF586003	HF585788
Ilanga cf. norfolkensis	MNHN IM-2007–18324	Chesterfield, New Caledonia	19°36'S, 158°43'E	568–570	EBISCO	Y	Y	HF586129	HF586270	HF585980	HF585814
Ilanga cf. norfolkensis	MNHN IM-2007–18325	Chesterfield, New Caledonia	19°36'S, 158°43'E	568–570	EBISCO	Y	Y	HF586130	HF586271	HF585981	HF585815
Machaeroplax delicatus	YK1484	Off Cape Toi, Kyushu Island	31°07'N, 131°39'E	1063–1082	R/V Tansei-maru, KT-11–12	N	?	HF586197	HF586342	HF586048	HF585896
Microgaza rotella	MNHN IM-2013–8023	Guadeloupe	16° 24'N, 61° 33'W	130	KARUBEN-THOS 2012/GD33	Y	Y	LT575964	LT575902	LT575920	LT575947
Microgaza rotella	MNHN IM-2013–8051	Guadeloupe	16° 24.97'N, 61° 33.8'W	85	KARUBEN-THOS 2012/GD31	Y	Y	LT575965	LT575898	LT575918	LT575946
Microgaza rotella	MNHN IM-2013–9016	Nord Pointe des Chateaux, Guadeloupe	16° 16.42'N, 61° 10.22'W	100	KARUBEN-THOS 2012/GD70	Y	Y	LT575966	LT575900	LT575921	LT575945
Microgaza rotella	MNHN IM-2013–20336	Le Moule, Guadeloupe	16° 19.9'N, 61° 19.47'W	1	KARUBEN-THOS 2012/GM14	Y	Y	LT575963	LT575899	LT575917	LT575943
Microgaza rotella	MNHN IM-2013–31167	Guadeloupe	16°25'N, 61°33'W	120	KARUBEN-THOS 2012/GN22	Y	Y	LT575967	LT575901	LT575919	LT575944

(*Continued*)

Table 1. Continued.

Species	Reg	Locality	Lat/Long	Depth (m)	Expedition/ Station	P	A	28S	COI	16S	12S
Minolia nyssonus	YK1355	E. Daiozaki, Honshu Island, Japan	34°17'N, 137°10'E	263	T/V Seisui-Maru, 96–05	Y	Y	HF586152	HF586294	HF586004	HF585838
Minolia n.s.	T10	Off Zyogashima, Kanagawa, Japan	–	–	–	Y	Y	HF586153	HF586296	HF586005	HF585839
Minolia punctata		Off Misaki, Kanagawa, Japan	35°09'N, 139°35'E	80	–	Y	Y	HF586155	HF586297	HF586007	HF585841
Solariella 6	MNHN IM-2007–18537	Russel Island, W.Bay, Solomon Is	9° 1.1' S, 159° 05.7' E	100–200	SALOMON2/ DW2169	Y	Y	–	HF586338	–	HF585891
Solariella affinis	NHMUK 20120233	Møre og Romsdal county, Vanylven, Rovdefjorden, Norway	62°11.45'N, 5°34'E	150–200	R/V 'Harry Borthen'	Y	Y		HF586321	HF586029	HF585872
Solariella chodon	MNHN IM-2007–18348	Boholi Island, Cortes, Philippines	9°43.3'N, 123° 48.8'E	123–135	PANGLAO2004	Y	Y	HF586180	HF586325	HF586033	–
Solariella obscura	SMNH-106159	Matochkin Strait, Russia	73°30'N, 57°50'E	9	Jenissej 1875/76	Y	Y	–	–	–	–
Solariella obscura	SMNH-106161	W of Novaya Zemlya, Arctic Ocean	79°37'N, 52°30'E	36	Jenissej 1875/52	Y	Y	–	–	–	–
Solariella segersi	MNHN IM-2007–18422	Bohol, off Balicasag Island, Philippines	9°28.4'N, 123°50.1'E	128–142	PANGLAO2005	Y	Y	HF586177	HF586322	HF586030	HF585875

(*Continued*)

Table 1. Continued.

Species	Reg	Locality	Lat/Long	Depth (m)	Expedition/ Station	P	A	28S	COI	16S	12S
'Solariella' varicosa	NHMUK 20120235	Finnmark county, Varangerfjorden, SW of Vestre Jakobselv, Norway	70° 4.00' N, 29° 12.00' E	10–174	R/V 'Asterias'	Y	Y	–	–	–	HF585720
Solariella varicosa	SMNH-106152	Mossel Bay, W Spitsbergen, Svalbard	79°50'N, 15°30'E	13–16	Swedish Polar/ 143	Y	Y	–	–	–	–
Solariella varicosa	SMNH-106155	Mossel Bay, W Spitsbergen	79°60'N, 15°20'E	22	Swedish Polar/132	Y	Y	–	–	–	–
Spectamen 1	MNHN IM-2007–18351	W Pamilacan Island, Philippines	9°30'N, 123° 50'E	100–138	PANGLAO 2004/T39	Y	Y	HF586186	HF586331	HF586038	HF585881
Spectamen 2	YK1381	Takarajima Island, Japan	29°25'N, 127°18'E	183–184	T/V Nagasaki-Maru N295	Y	Y	HF586189	HF586335	HF586040	HF585885
Spectamen 4	WAM S25789	Off Bald Island, Australia	35°16.11'S, 118° 43.12'E to 35°17.17'S, 118°42.36'E	973–999	CSIRO RV 'Southern Surveyor'	Y	Y	HF586175	HF586319	HF586027	HF585869
Spectamen laevior	MNHN IM-2007–18428	Bohol Sea, Philippines	9°28.4'N, 123°50'E	128–142	PANGLAO 2005/CP2344	Y	Y	HF586187	HF586332	HF586039	HF585882
Spectamen mutabilis	**MNHN IM-2009–28738**	**Philippines**	**14° 46' N, 123° 40' E**	**357–367**	**AURORA/ CP2695**	Y	Y	**HF586188**	**HF586334**	**–**	**HF585884**

(*Continued*)

Table 1. Continued.

Species	Reg	Locality	Lat/Long	Depth (m)	Expedition/ Station	P	A	28S	COI	16S	12S
Spectamen philippensis	NHM 201104524	North Morton Island, Australia	26°56.6'S, 153° 24.3'E	31	–	Y	Y	HF586176	HF586320	HF586028	HF585870
Suavotrochus sp	YK1382	W. Namami Island, Japan	28°36'N, 127°04'E	704–730	T/V Nagasaki-Maru N295	N	?	HF586198	HF586343	HF586049	HF585897
Zetela 1	MNHN IM-2009–15167	Mozambique Channel	25°13'S, 35°21'E	700–707	MAINBAZA/ CP3138	Y	?	HF586194	HF586339	HF586045	HF585786
Zetela 1	MNHN IM-2009–15169	Mozambique Channel	25°13'S, 35°21'E	700–707	MAINBAZA/ CP3138	Y	?	–	HF586340	HF586046	HF585893
***Zetela* 1**	**MNHN IM-2009–8748**	**Mozambique Channel**	**25° 13' S, 35° 21' E**	**700–707**	**MAINBAZA/ CP3138**	**Y**	**?**	**HF586195**	**HF586341**	**HF586047**	**HF585895**
Zetela 2	NHMUK 20120236	Eastern Weddell Sea, Antarctica	71° 18.35' S, 13° 57.71' W	1030	ANDEEP III/ PS67/074-6-E	Y	Y	HF586050	HF586199	HF585898	HF585714
Zetela 2	BAS KL05-0328	Antarctica	71° 18.35' S 13° 57.71' W	1030	ANDEEP III/ PS67/074–6-E	Y	Y	–	–	–	–
Zetela 3	NHMUK 20120240	Burdwood Bank, Antarctica	54° 30.22' S, 56° 8.20' W	286–290	LAMPOS ANDEEP/150–1	Y	Y	HF586054	HF586204	HF585903	HF585719
Zetela alphonsi	ZSM 20041246	Región del BioBío, Chile	36°24.1'S, 73°36.4'W	600	–	N	?	–	–	–	–
Zetela alphonsi	ZSM 20041458	Región del BioBío, Chile	36°24.1'S, 73°36.4'W	600	–	N	?	–	–	–	–
Zetela alphonsi	**ZSM-MOL-20041247**	**Región del BioBío, Chile**	**36°24.1'S, 73°36.4'W**	**600**	**–**	N	**N**	**–**	**–**	**–**	**–**

Eye morphology data, P, pigmentation present (Y), absent (N), or unknown (?); A, eye aperture open (Y), obscured or closed (N), or unknown (?). Specimens in bold were used in histological studies.

transversion/transition of 1:4:1) for all sequences and were run for 30,000,000 generations with a sample frequency of 1 tree per 1,000. The first 25% of trees were discarded, so that the final consensus tree was computed from a total of 22,500 trees.

Ancestral state reconstructions for eye characters were performed in Mesquite (Maddison and Maddison 2015) using parsimony and Maximum Likelihood to calculate most parsimonious character states and proportional likelihoods for character states at each node of the time-calibrated tree produced in BEAST. Likelihood ratio testing indicated that single rate Markov (Mk1) models provided the best fit for eye pigmentation, size, and status of the vitreous body, and that a two-rate asymmetric model (Mk2) was more appropriate for the status of the eye aperture in Maximum Likelihood reconstructions.

GROSS MORPHOLOGY

We examined 114 individual specimens of 67 different species (Table 1) using as many deep-sea species as possible from across the family; all available genera were sampled (see above for taxon selection). Nondestructive examinations of the eyes under a dissecting microscope were sufficient to determine the presence or absence of pigment and, where pigment was present, the status of the eye aperture and any tissue obscuring it. These two characters were used as broad indicators of eye loss so as to track its presence throughout the family.

HISTOLOGY AND DIGITAL RECONSTRUCTION

The left eye and surrounding tissue was removed from the nine specimens selected for histological studies. For material stored in ethanol (all specimens except *Z. alphonsi*), tissue required gradual rehydration through a decreasing ethanol series (3 × 15 minutes in 90, 70, 50, and 30% ethanol and pure distilled water). Samples were postfixed in 1% osmium tetroxide in distilled water for 2 hours, washed in distilled water and dehydrated in an increasing acetone series. The specimen of *Z. alphonsi* was fixed in 2.5% glutaraldehyde in cacodylate buffer (0.1 M, pH 7.4), osmicated in 1% osmium tetroxide in cacodylate buffer, washed in dilute cacodylate buffer, and dehydrated in acetone as before, after Ruthensteiner (2008). Tissue was embedded in Epon epoxy resin with DPM-30 accelerator for 48 hours at 65°C, according to the manufacturer's instructions (Sigma Life Sciences).

Samples were serially sectioned at a thickness of 1.5 μm using a diamond knife (HistoJumbo 8 mm, DiATOME 8 mm, Switzerland) on an automated microtome (Leica RM2255) and stained using Richardson's solution (Richardson et al. 1960). Images of sections were digitally recorded using an Olympus E-600 digital camera mounted on an Olympus BX41 light microscope at a magnification appropriate to each sample. The images were reduced and contrast-enhanced for reconstruction using Adobe Photoshop CS4. Images were aligned into stacks using AMIRA v5.3.3 (Visualization Sciences Group) and anatomical features of the eye were identified throughout the image stacks before surface rendering and smoothing to produce 3D tomographic models.

Results

Eye reduction was evident in 20 of the 67 species studied overall. Morphological changes observed through gross morphology and histology included loss of pigmentation, obstruction of the eye aperture, reduction or fragmentation of the vitreous body, and overall reduction in eye size. In the context of the phylogenetic reconstruction, we estimate that eye reduction has evolved at least seven times (and in at least seven genera) in Solariellidae, along variable morphological pathways.

PHYLOGENETIC AND ANCESTRAL STATE RECONSTRUCTION

A time-calibrated combined-gene tree generated in BEAST resolved clear genus-level clades with generally high support, and we present it here as a fully resolved tree (Fig. 4). The topology is similar to that resolved by Williams et al. (2013): the same ten clades corresponding to genera were also recovered in this study, along with, *Microgaza rotella*, a genus not represented in the previous study, and "*Bathymophila*" 18, which falls outside *Bathymophila* despite appearing morphologically to belong therein. As in Williams et al. (2013) "*Suavotrochus*" sp. and "*Machaeroplax*" *delicatus* do not resolve within any of these genus-level clades. Relationships among these clades generally had high statistical support (node support values greater than 97% for all but three relevant nodes). There were two key topological differences from previous analyses by Williams et al.: the placement of (*Archiminolia* + *Arxellia*) in a larger grouping (*Bathymophila*+ ("*Bathymophila*" 18+ (*Archiminolia* + *Arxellia*)), though this is not well supported (Fig. 4), and the nonrecovery of a clade ((*Zetela*+ Clade B) + (*Minolia* + *Hazuregyra watanabei*)), which was only poorly supported in Williams et al. (2013). Within-clade (species level) relationships are almost identical to those resolved by Williams et al. (2013) where sampling is consistent with that study. The combined-gene trees produced in MrBayes (SD1) showed well-resolved generic-level clades in agreement with previous results (Williams et al. 2013), which further support the combined-gene BEAST analysis. In Bayesian analyses under MrBayes, within-clade relationships were identical except for the relative positions of *Spectamen mutabilis* and *S. laevior.* Relationships between clades were not well resolved. The *Ilanga* and (*Elaphriella* + (*Machaeroplax* + *Suavotrochus*)) clades were resolved as the two earliest diverging groups, but MrBayes analyses recovered separate Clade B and *Zetela* groups diverging next (though with lower support than the

alternative relationships found in BEAST) (SD1). Individual gene trees clearly resolved species-level clades (SD2,3).

In MrBayes analyses the average standard deviation of split frequencies approached zero, all parameter average PSRF values were ≤ 1.003 and in these Bayesian analyses minimum ESS values in combined runs exceeded 200 for all parameters. Visual examination of traces showed that all parameters reached stationarity and converged between independent runs for each dataset.

Parsimony analyses further support the BEAST and MrBayes trees, and no additional information regarding topology was recovered. In line with the previous work of Williams et al. (2013), we therefore illustrate the results of BEAST analyses as our preferred tree and the basis of further inference (Fig. 4).

Within-clade relationships and several between-clade relationships were particularly well supported by consensus across all analyses and methods, such as the groupings of *Solariella* and *Spectamen, Arxellia, Archiminolia*, and "*Bathymophila*" 18, and *Microgaza, Minolia,* and *Hazuregyra.* Where topological conflicts occurred we referred to the better-supported higher level topology resolved by the BEAST tree to generate ancestral state reconstructions for assigned eye characters (SD4).

GROSS MORPHOLOGY

Solariellids fall into three distinct groups of eye morphs (Figs. 2, 3). Of the 67 species studied, 47 have typical pigmented eyes of normal size with an open aperture, and at least one of these morphs were found in all genera examined, except in *Machaeroplax* and *Suavotrochus* (Fig. 4, Table 1). Fifteen species across at least seven genera (*Archiminolia, Elaphriella, Suavotrochus, Machaeroplax, Zetela, Bathymophila,* and "*Bathymophila*" 18; generic level placement of the latter is uncertain) lack pigmented eyes (Fig. 4, Table 1). The status of the eye aperture and size of the eye are not visible in these specimens without histology. Five species in two genera (*Bathymophila* and *Elaphriella*) retain their pigmentation but the eye aperture is obscured by a layer of tissue covering the eye, which is of a normal size (Fig. 4, Table 1). One species, *Zetela* 1, has unusual eyes of which the proximal half is pigmented and the distal half is not, so the aperture (if present) is not visible. This was observed in all three specimens studied. In the context of our phylogenetic and ancestral state reconstructions, we conclude that eye reduction (the novel appearance of one or more reduced characters in a previously fully eyed lineage) has evolved at least seven times independently in Solariellidae; at least twice in *Bathymophila* (sensu Williams et al. 2013), and at least once in each of *Archiminolia, Elaphriella, Zetela,* and (*Machaeroplax* + *Suavotrochus*) (Fig. 4).

HISTOLOGY AND DIGITAL RECONSTRUCTION

Among the nine species studied histologically, we identified five different eye anatomies. Structurally typical vetigastropod eyes were confirmed in three species: *Ilanga* 6, *Ilanga* 10, and *Spectamen mutabilis* all have fully formed pigmented eyes on short eyestalks posterior of the base of the cephalic tentacle (Fig. 2). The vitreous body is large, round, and intact, microvilli are well organized and of uniform length, and photoreceptors are interspersed between the pigment cells of the retina (Fig. 3A, SD5.1, SD5.2, SD5.3). The eye aperture is open and unobstructed, and the optic nerve can be traced from the retina to the cerebral ganglion. There are minor anatomical differences between these three species; the eye of *Ilanga* 10 appears to be slightly compressed with microvilli of variable lengths, and the eye of *S. mutabilis* has an unusually wide aperture (53 μm, eye diameter 85 μm), the vitreous body is slightly reduced in size and microvilli are very long.

A layer of tissue covers the eye in two species: *Bathymophila diadema* and *Elaphriella khantaros* (Fig. 3B, SD5.4). A layer of external epithelium, the closed retinal epithelium and, in all but a very small central area, some interstitial tissue cover the eye and obstruct the aperture. In this central area, the retina passes very close to the surface epithelium and may fuse with it, but there is no opening (Fig. 3B). In both species, the retina is pigmented and cells are well-organized, with many photoreceptors and a strong connection to the optic nerve (Fig. 3B, SD5.4). Again, there are obvious differences between the two species. There appears to be less pigmentation in the retina of *B. diadema* than in other species (e.g., *Ilanga,* Fig. 3B) and the vitreous body, though present, is small and fragmented and microvilli are elongated. Some of the optic cup appears to be empty (Fig. 3B). In *E. khantaros* the vitreous body is large and intact and microvilli are irregular lengths.

Reduced eyes, which were invisible from the surface due to loss of pigmentation, were found in "*Bathymophila*" 18 (Fig. 3D, SD5.5). The vitreous body is fragmented and reduced, and few ciliary photoreceptors are visible. The eye of "*Bathymophila*" 18 was very small (diameter 55 μm, body length 5 mm), with the retina only counting 14 cells across at its widest point, whereas the smallest specimen overall, *S. mutabilis* (body length 4 mm), had a retina at least 22 cells across (eye diameter 85 μm). The eye aperture appeared to remain open and uncovered in both species, but was very narrow (5 μm) in "*Bathymophila*" 18 (Fig. 3D) compared to the more typical eyes of *Ilanga* 6 (aperture 70 μm, eye diameter 250 μm). The eye remains well connected to the optic nerve, which is large and reaches the cerebral ganglion intact (SD5.5).

Unpigmented eyes were also observed in *E. wareni* and *Z. alphonsi*, but in these species the eye aperture was covered by a layer of tissue in a fashion reminiscent of *B. diadema* and *E. khantaros* (Fig. 3C, SD5.6). In addition, the vitreous body appears to be entirely absent in *E. wareni*, and microvilli are elongated and irregular. Some ciliary projections of photoreceptors are present. The optic nerve surrounds the optic cup and is larger at the distal

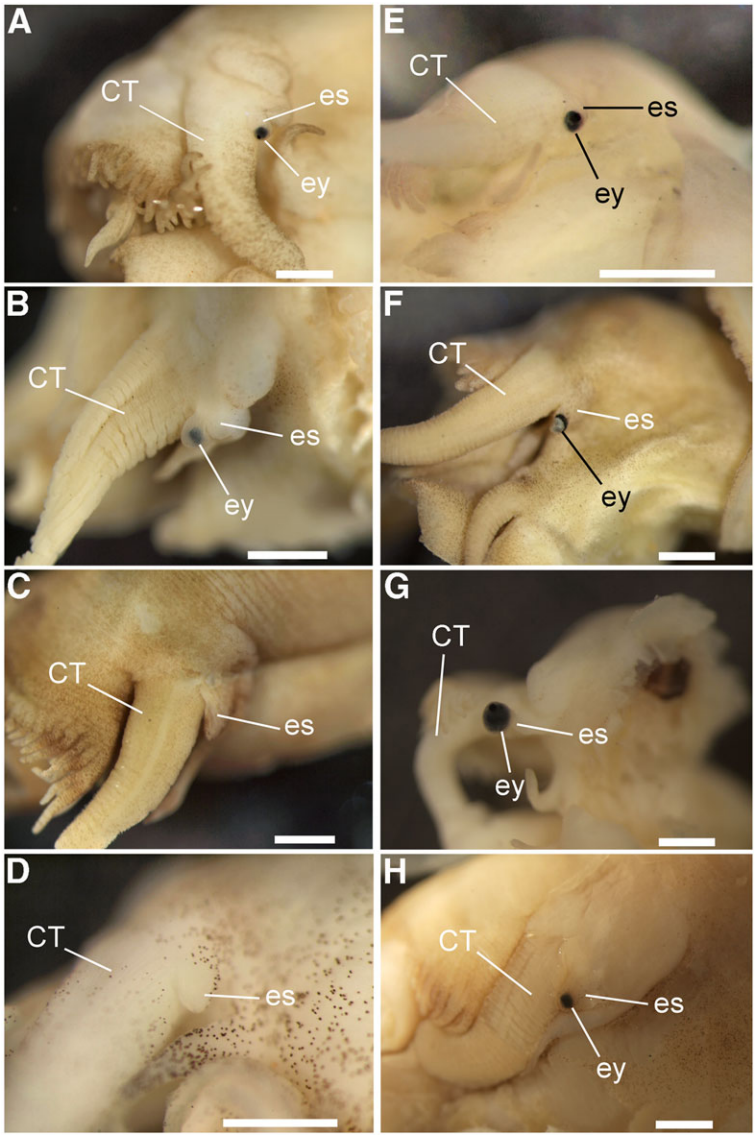

Figure 2. **Eye morphology in solariellid species studied histologically. Variety in eye morphology is evident in different species even from external examination, as shown here. (A) *Ilanga* 10 (typical eye); (B) *Bathymophila diadema* (with eye covered by skin); (C) *Elaphriella wareni* (lacking pigment); (D) "*Bathymophila*" 18 (lacking pigment). (E) *Spectamen mutabilis* (typical eye); (F) *Zetela* 1 (half pigmented, atypical shape); (G) *Ilanga* 6 (typical eye); (H) *Elaphriella khantaros* (with eye covered by skin); CT, cephalic tentacle; es, eyestalk; ey, eye. Scale bars, 500 μm.**

(eye) end; it connects to the cerebral ganglion as in other species but it narrows considerably toward the proximal (brain) end (Fig. 3C, SD5.6).

Partially pigmented but apparently misshapen eyes were found in *Zetela* 1. This species has straight, slender eyestalks with the eye protruding from the tip (Fig. 2D). The eye does not represent the typical cup shape observed in other species, instead being ball-shaped and without an aperture, and not surrounded by other tissue (nerve tissue is only visible at the very base) (SD5.7). The proximal part of the retina is pigmented, but the distal side is not. Modeling revealed a dent-like disfigurement in the shape of the eye, which was also seen, but to a lesser extent, in the other specimens of the same species (SD5.7). The vitreous body was visible in few sections and appears to be small, with a large volume of long microvilli filling the proximal part of the eye and a large part of the distal side being empty (SD5.7).

Discussion

The number and variability of eye reductions found within Solariellidae indicate that although there is evidence of strong selective pressure in favor of eye loss in dark-living animals (Jones

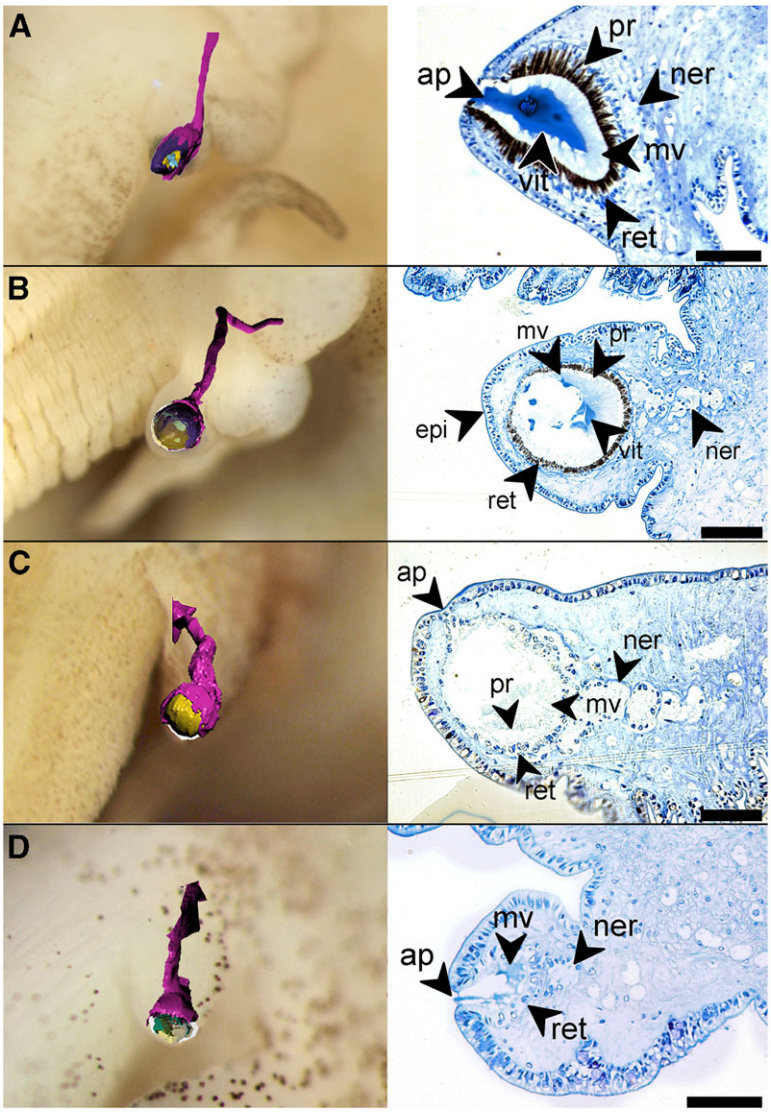

Figure 3. Variety in solariellid eye anatomy. Semithin sections, taken through the eye along a sagittal plane as in Figure 1, and tomographic modeling demonstrate the full extent of variety of eye structures and deviations from the typical eye (Fig. 1) in different species. Left, photograph with superimposed tomographic model of eye structure; right, section through the eye. Four species as in Figure 2; also compare phylogenetic positions in Figure 4. (A) *Ilanga* 10; (B) *Bathymophila diadema*; (C) *Elaphriella wareni;* (D) "*Bathymophila*" 18. Ap, eye aperture; epi, epithelium; mv, microvillous layer; ner, optic nerve; pr, photoreceptors; ret, retina. Scale bars, 50 μm.

and Culver 1989), the anatomical trajectory of its evolution is not predictable or consistent even amongst closely related species. These findings have important implications for understanding the biology of this gastropod family but also as a case study for the evolution of the loss of complex traits such as eyes (Serb and Eernisse 2008).

EYE LOSS AND EVOLUTION IN SOLARIELLIDAE

Eye reduction is more widespread than previously reported amongst deep-sea solariellids, and we documented many new cases here (Williams et al. 2013). The frequency of apparently independent eye reduction and loss events with variable anatomical forms has positioned Solariellidae as an important group for the study of "reductive" evolution. The group contains many undescribed species and more continue to be discovered (Marshall 1999; Vilvens 2002; Williams et al. 2013; Vilvens et al. 2014; Vilvens and Williams 2016). As well as recording the presence or absence of retinal pigmentation in additional species, we also introduced a new metric, the presence or absence of the eye aperture, which can in many cases be determined without invasive examination. Combined with pigmentation data, this indicated that eye reduction is much more widespread than previously reported, occurring in at least six of the 14 solariellid genera (the placement of "*Bathymophila*" 18 is unclear; Fig. 4). Even in groups

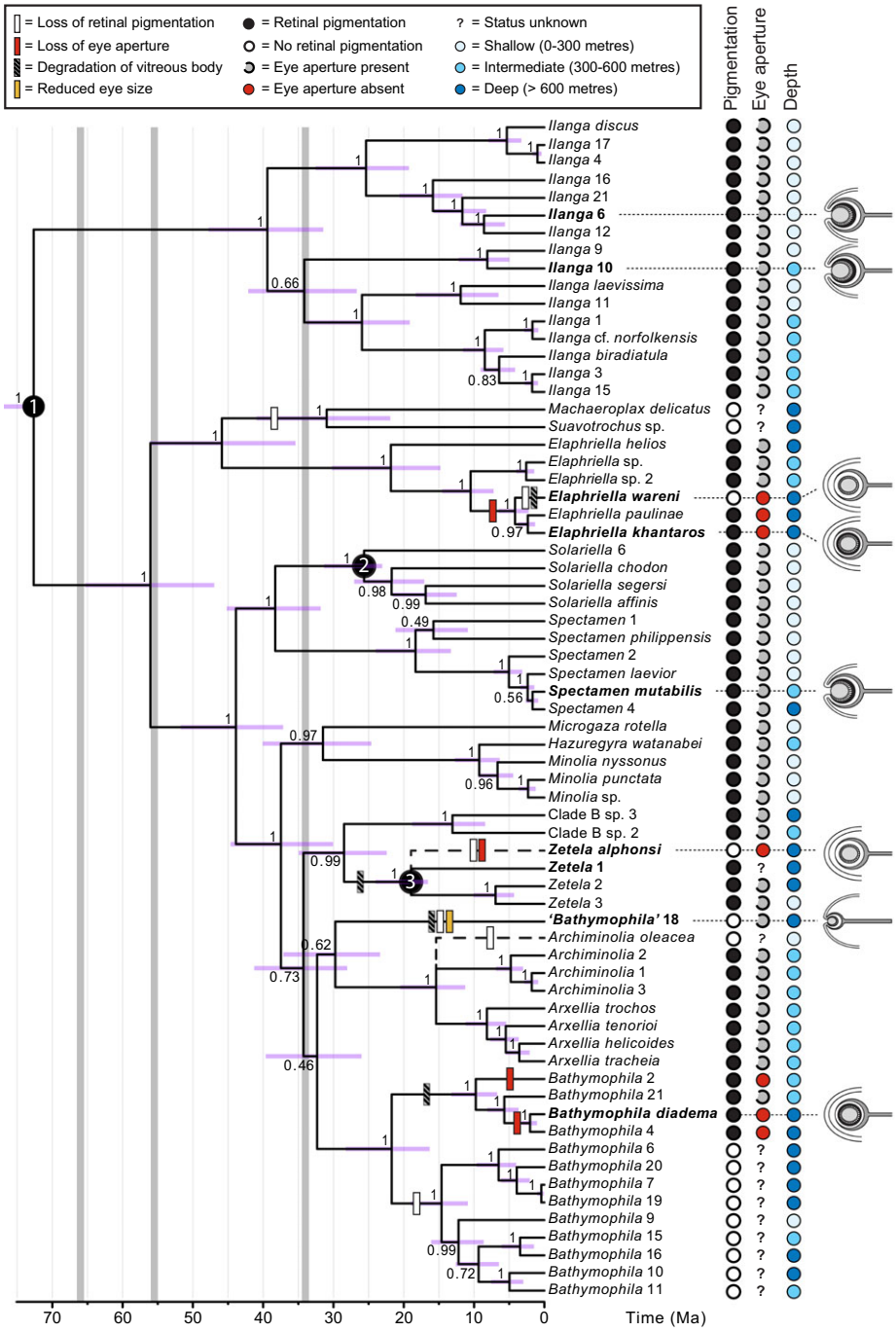

Figure 4. Time-calibrated solariellid phylogeny mapping eye morphs, species depth range, and proposed occurrence of eye reduction events in all examined species. Branch lengths are proportional to time (scale below in millions of years) based on the BEAST reconstruction. Node support values are posterior probabilities. Light horizontal bars on nodes correspond to 95% highest posterior density (HPD) interval for node ages (i.e., the shortest interval that contains 95% of the sampled values). Three time calibrations are indicated: 1, ingroup calibration; 2, *Solariella* calibration, 3, *Zetela* calibration; see Williams et al. (2013) for further details. Species in bold were studied histologically and a schematic diagram of eye anatomy is shown. Remaining species were examined externally. Two species noted with dotted lines, *Archiminolia oleacea* and *Zetela alphonsi*, were not included in molecular analyses and occupy unresolved positions in their accepted genera. Events are plotted at the earliest point where the reduced state is the most parsimonious or where proportional likelihood at the succeeding node is greater than 0.95 for the reduced state. Tree topology follows the BEAST tree, with a single specimen representing each species. Vertical gray bars represent important geological events: Cretaceous-Tertiary boundary (66 Ma), Palaeocene-Eocene thermal maximum (55.5 Ma), and Eocene-Oligocene transition (34 Ma).

beyond Vetigastropoda where there is no exposed eye aperture, the use of covering or sinking of the eye itself can be used as a comparable metric for eye reduction. The lack of pigmentation in the retina of *Archiminolia oleacea* is unusual, as it mostly inhabits intermediate depths and this feature has not been reported previously, though it has potential taxonomic importance because *A. oleacea* is the type species of the genus. Both *A. oleacea* and *Z. alphonsi* may be unique in their genera for lacking retinal pigmentation, with congeneric species descriptions either noting the presence of pigmented eyes, or omitting description of the eyes altogether. In *Bathymophila* it is possible that the loss of eyes in both clades coincided with their rapid diversification after expansion into deeper water as suggested by Williams et al. (2013). Similar increases in diversification rate have been observed in eyeless deep-water clades of ostracods, compared to sighted shallow-water clades (Syme and Oakley 2012). Conversely, some deep-sea species in this family appear to have retained intact eyes despite a substantial evolutionary history of inhabiting deep water, such as *Bathymophila* 21 and Clade B sp.2 (Williams et al. 2013). Further investigation of ocular ultrastructure in more species, especially those with apparently degenerate eyes (*Bathymophila* spp., *A. oleacea*, *E. paulinae*, *Suavotrochus*, *Machaeroplax*) is warranted to determine whether they show other signs of eye reduction as well. The status of characters such as the eye aperture can only be determined through histological sampling.

Most importantly, this study demonstrates that the evolutionary route to eye loss is highly variable even among these closely related species. Reduction events such as loss of pigmentation, degradation of the "lens" and covering of the eye aperture can occur independently. This is strong evidence that such individual features do not appear in any particular order in a trajectory toward eye loss. While the eyes of some species (*B. diadema, E. khantaros*) have become enveloped by the surrounding epithelium, they retain their retinal pigmentation. Conversely, others have nonpigmented eyes that remain unobstructed ("*Bathymophila*" 18). Degeneration of the vitreous body has occurred in some, but not all, otherwise apparently similar eye morphs (*B. diadema* has a fragmented vitreous body but *E. khantaros* does not), and overall reduction in size is observed in only one species ("*Bathymophila*" 18). Our ancestral state reconstructions support this conclusion and indicate that the features we have identified can occur in different orders. Further additions to our histological dataset will help to clarify the evolutionary history of these traits and further reduce uncertainty in the character reconstruction. It is clear from the data presented here that even in closely related species there is no evidence for a consistent order of events. This is demonstrated not only by the fundamentally different structural changes that have occurred in *E. khantaros* and "*Bathymophila*" 18, for example, but also by the two contrasting morphologies within *Bathymophila* (sensu Williams et al. 2013) despite their taxonomic proximity (Figs. 3, 4). Without secondary regain of features, which we consider to be unlikely, these different morphological pathways are simply mutually exclusive. Additionally, this conclusion is also robust to any remaining phylogenetic uncertainty in the fully resolved BEAST tree: we have confirmed species identity of all specimens (SD2,3) and recovered relationships within clades that are supported by previous and supporting analyses (SD1; Williams et al. 2013). The key anatomical divergences that support our conclusion are found at taxonomic levels unaffected by phylogenetic uncertainty at deeper nodes.

BROADER IMPLICATIONS FOR THE EVOLUTION OF EYE LOSS

The variety in evolutionary trajectory apparent in Solariellidae indicates there is unlikely to be a universal developmental cause of eye reduction, even between closely related species. Studies of the cavefish *A. mexicanus* have shown that the lens, and the apoptosis of cells therein, controls subsequent degeneration events, resulting in many of the convergent morphological features seen in independent eyeless populations (Jeffery 2005). Alterations to lens apoptosis during development are also implicated in the eye degeneration of two *Rhamdia* cave catfishes (Wilkens 2001). However, given the variety of pathways to reduction found in solariellids, it is unlikely that there is a similar developmental "master key" that affects eye development downstream in this group. In the future, we propose that visual anatomy in Solariellidae or other gastropod or molluscan groups could provide valuable new model systems for wider evolutionary studies (Serb and Eernisse 2008).

Histological investigations show structural features that deviate from the "typical" solariellid eye in seven of nine species examined, which in many cases were not visible from superficial examinations. Not only the loss of pigmentation, but the covering of the eye by epithelial tissue, disintegration of the vitreous body and reduction in size are all classic characters associated with eye reduction in dark environments (Culver 1982). The elongation of microvilli and widened aperture seen in *S. mutabilis* may contribute to increasing light capture and heightening visual sensitivity in dim, intermediate-depth environments (Warrant et al. 2003; Land and Nilsson 2012; Malkowsky and Götze 2014).

There are of course typical character states that are found at some stage during the evolution of eye loss in this case: loss of pigmentation, disintegration of the vitreous body and covering of the eye have evolved recurrently in taxa undergoing eye reduction independently. This trend is well-known and extends beyond the taxonomic scope of this study; these same reduction events have been reported in many other animal groups

(Culver 1982; Jones et al. 1992). However, by atomizing the overall process of eye loss, we found that the order of their occurrence is not consistent and thus individual "reduced" phenotypes can be very different. Pigmentation is not the ultimate indicator of eye function, though it has been used as such a proxy for many years. Here we have shown that many species deviate significantly from the typical form without losing pigmentation, and this suggests that similar cases may have been missed in other groups. By mapping anatomical data on our resolved tree, it is clear that the reduction of specific anatomical features represent different processes taking place in parallel, and thus the presence or absence of pigmentation does not necessarily reflect other aspects of eye structure (Fig. 4). Histological studies, though time consuming, are necessary to properly understand what is happening beneath the surface. Certain characteristic features of reduction that we expected to observe do not appear to have occurred at all, including degeneration of the nerve tissue. Although this is considered a classic sign of eye redundancy (Culver 1982; Langecker and Longley 1993), the absence of neural degeneration has also been observed in blind cave fishes (Wilkens and Strecker 2003) and it has been suggested that dysfunctional eyes could be adapted or modified to detect other stimuli such as chemical cues, accounting for the persistence of the optic nerves (Brinton 1987).

Indeed, the putative potential for energetic reinvestment in other sensory systems is one possible evolutionary advantage of eye reduction: as well as losing their eyes, many cave animals have elongated limbs and antennae, and increased sensitivity to tactile and chemical cues (Culver 1982; Iliffe and Kornicker 2009). In the case of solariellids and other vetigastropods, a pair of cephalic tentacles originates from the head from the same point as the eyestalks, with paired accessory tentacles posterior and usually ventral to this. These cephalic tentacles are often thicker in deeper-water solariellid taxa (STW, pers. obs.). More detailed examination of these tentacles and their innervation may shed some light on the relative investment balance between vision and mechano- or chemoreception in the tentacles. Given the intermediate state of eye loss observed in several species, this could help determine whether the eyes themselves are still functional in any rudimentary way or whether an energetic tradeoff is occurring, in the absence of live observations. However, Culver et al. (1995) suggest that these "constructive" traits may arise more slowly than the "regressive" loss of eyes as a result of the faster action of combined neutral evolution and selection on eye-related genes compared to selective pressure alone on other sensory modalities, and we did not observe any dramatic differences in tentacle morphology between eyed and eyeless species.

Where eye reduction evidentially has evolved in very different ways, it is possible that other evolutionary constraints affect its trajectory. In talpid moles, for example, eye reduction is thought to have been significantly influenced by ecology and biomechanics of burrowing techniques (Borghi et al. 2002). Some deep-sea fishes with overlapping depth ranges exhibit different extents of eye degeneration, also likely as a result of different ecological pressures and behavior (Munk 1964). Depth does appear to be a fairly good indicator for eye reduction overall in the current study, with only four of the twenty deep-water species (600 metres and deeper) apparently having typical eyes, but several species inhabiting similar depths and regions differ dramatically in their eye structure. This also includes *Archiminolia oleacea* and *Bathymophila* 9, which exhibit pigment loss even at shallow depths (though this is likely to be ancestral to the *Bathymophila* clade). Ecological or behavioral differences such as feeding habits, major predators or residual eye functionality may wholly or partially account for some of these variations, but due to the rarity and inaccessibility of these species and the absence of live observations, we lack further data that may be necessary to take into account.

Both directional selection and neutral mutation have important roles to play in the evolution of eye loss, with the former apparently driving for the reduction of eyes overall (Jones and Culver 1989), and the latter, or a combination of the two, likely generating the random order of reduction events that we see here (Fong et al. 1995; Wiens et al. 2003); however disentangling their relative contributions remains a considerable challenge. Although evolutionary process cannot be directly inferred from the patterns we observe here, they appear to be congruent with a significant role for the release of evolutionary constraint. Our findings do emphasize the importance of terminology regarding regressive evolution; many authors describe "convergent evolution" of eye reduction in dark-dwelling species (e.g., Derkarabetian et al. 2010; Hedin and Thomas 2010). However, although the reduction of eyes occurs frequently, it appears that both the evolutionary mechanisms by which it evolves and the resulting anatomy are not necessarily convergent. It is important to distinguish between the process and the resulting character, as this affects the implications of interplay between selection, neutral mutation, and pleiotropy. For example Brinton (1987) and Zharkova (1970) described four stages of eye loss in deep-sea crustaceans, Jäger (2012) discovered several species of troglobitic spider that displayed "gradually increasing troglomorphic features," and Malkowsky and Götze (2014) found convergent patterns in the eye structure of scallops living in aphotic zones and referred to the evolution of eye reduction in this case as "successive." However, these studies did not consider the overlap of occurrence of specific reduction features, despite implying predictability in their results. These systems represent untested hypotheses, where phylogeography could be compared to anatomy to determine whether there is or is not a conserved anatomical trajectory to eye reduction.

Conclusions

This study was restricted to a single family and compared closely related species. Many of them overlap geographically and in depth range, and are potentially exposed to comparable selective pressures. One might expect their identical conditions, simple and well-conserved eye structure and shared morphological constraints to have produced similar reduced eye morphologies. However, we found evidence against a conserved pathway for eye reduction, with dramatic differences in reduction morphology occurring even within a single morphogenus. There is greater plasticity in this process than has previously been appreciated, and we consider it highly unlikely that eye loss occurs through a common or most likely morphological trajectory, certainly within Mollusca and most likely throughout Metazoa.

ACKNOWLEDGMENTS

We gratefully acknowledge Philippe Bouchet (MNHN), who kindly provided many of the specimens used in this study. MNHN material was collected during expeditions of the "Tropical Deep-Sea Benthos" programme under PIs Bertrand Richer de Forges, Philippe Bouchet, and Sarah Samadi: AURORA, BENTHAUS, BERYX, BIOPAPUA, BOA 1, BORDEAU 1, CONCALIS, EBISCO, NORFOLK 1 and 2, PANGLAO 2005, SOLOMON 1 and 2, TAIWAN 2001, and TERRASSES. The Principal Investigators acknowledge Institut de Recherche pour le Développement (IRD), the Philippines Bureau of Fisheries and Aquatic Resources (BFAR), and National Taiwan Ocean University (NTOU) for ship time. Additional material was collected during the MNHN-PNI "Our Planet Reviewed" expeditions: MAINBAZA, MIRIKY, PANGLAO 2004, and SANTO 2006, for which Philippe Bouchet acknowledges the support of the Total Foundation and Prince Albert II of Monaco Foundation. For the context of the expeditions, see Bouchet et al. (2008) and http://expeditions.mnhn.fr/?lang = en_US. We also thank Enrico Schwabe and Martin Heβ (ZSM, LMU) for discussions leading to the design of this project and for the use of specimens of *Zetela alphonsi*, Bruce Marshall (NMNZ) for his assistance with specimens of *Archiminolia oleacea,* Jessica Sells (NHM) for her assistance in the laboratory and the staff of Queen's University Marine Laboratory (QUB) for their technical assistance. We are also very grateful for the valuable comments and feedback of three reviewers.

DATA ARCHIVING

Data available from the Dryad Digital Repository: http://dx.doi.org/10.5061/dryad.d1k3b

LITERATURE CITED

Aspiras, A. C., R. Prasad, D. W. Fong, D. B. Carlini, and D. R. Angelini. 2012. Parallel reduction in expression of the eye development gene *hedgehog* in separately derived cave populations of the amphipod *Gammarus minus*. J. Evol. Biol. 25:995–1001.

Baker, A. J., O. Haddrath, J. D. McPherson, and A. Cloutier. 2014. Genomic support for a Moa-Tinamou clade and adaptive morphological convergence in flightless ratites. Mol. Biol. Evol. 1–11.

Borghi, C. E., S. M. Giannoni, and V. G. Roig. 2002. Eye reduction in subterranean mammals and eye protective behaviour in *Ctenomys*. Mastozoología Neotrop. J. Neotrop. Mammal. 9:123–134.

Brinton, E. 1987. A new abyssal Euphausiid, *Thysanopoda minyops*, with comparisons of eye size, photophores, and associated structures among deep-living species. J. Crust. Biol. 7:636–666.

Castresana, J. 2000. Selection of conserved blocks from multiple alignments for their use in phylogenetic analysis. Mol. Biol. Evol. 17:540–552.

Culver, D. C. 1982. Cave life: Evolution and ecology. Harvard Univ. Press, Cambridge, MA.

Culver, D. C., T. C. Kane, and D. W. Fong. 1995. Adaptation and natural selection in caves: the evolution of *Gammarus minus*. Harvard Univ. Press, Cambridge, MA.

Darriba, D., G. L. Taboada, R. Doallo, and D. Posada. 2012. jModelTest 2: more models, new heuristics and parallel computing. Nat. Methods 9:772.

Darwin, C. 1859. Origin of species. John Murray, London.

Derkarabetian, S., D. B. Steinmann, and M. Hedin. 2010. Repeated and time-correlated morphological convergence in cave-dwelling harvestmen (Opiliones, Laniatores) from Montane Western North America. PLoS One 5:e10388.

Drummond, A. J., M. A. Suchard, D. Xie, and A. Rambaut. 2012. Bayesian phylogenetics with BEAUti and the BEAST 1.7. Mol. Biol. Evol. 29:1969–1973.

Edgar, R. C. 2004. MUSCLE: multiple sequence alignment with high accuracy and high throughput. Nucleic Acids Res. 32:1792–1797.

Fong, D. W., T. C. Kane, and D. C. Culver. 1995. Vestigialisation and loss of non-functional characters. Annu. Rev. Ecol. Syst. 26:249–268.

Guindon, S., and O. Gascuel. 2003. A simple, fast and accurate method to estimate large phylogenies by maximum-likelihood. Syst. Biol. 52:696–704.

Harvey, P. H., and M. D. Pagel. 1991. The comparative method in evolutionary biology. Oxford Univ. Press, Oxford.

Haszprunar, G. 1988. On the origin and evolution of major gastropods group, with special reference to the streptoneura. J. Molluscan Stud. 54:367–441.

Hedin, M., and S. M. Thomas. 2010. Molecular systematics of eastern North American Phalangodidae (Arachnida: Opiliones: Laniatores), demonstrating convergent morphological evolution in caves. Mol. Phylogenet. Evol. 54:107–21.

Hessler, R. R., and D. Thistle. 1975. On the place of origin of deep-sea isopods. Mar. Biol. 32:155–165.

Huelsenbeck, J. P., and F. Ronquist. 2001. MRBAYES: Bayesian inference of phylogenetic trees. Bioinformatics 17:754–755.

Iliffe, T. M., and L. S. Kornicker. 2009. Worldwide diving discoveries of living fossil animals from the depths of anchialine and marine caves. Smithson. Contrib. Mar. Sci. 38:269–280.

Jäger, P. 2012. Revision of the genus *Sinopoda* Jäger, 1999 in Laos with discovery of the first eyeless huntsman spider species (Sparassidae: Heteropodinae). Zootaxa 57:37–57.

Jeffery, W. R. 2005. Adaptive evolution of eye degeneration in the mexican blind cavefish. J. Hered. 96:185–196.

———. 2009. Regressive evolution in *Astyanax* cavefish. Annu. Rev. Genet. 43:25–47.

Jones, R., and D. C. Culver. 1989. Evidence for selection on sensory structures in a cave population of *Gammarus minus*. Evolution 43:688–693.

Jones, R., D. C. Culver, and T. C. Kane. 1992. Are parallel morphologies of cave organisms the result of similar selection pressures? Soc. Study Evol. 46:353–365.

Kano, Y., and T. Kase. 2002. Anatomy and systematics of the submarine-cave gastropod *Pisulina* (Neritopsina: Nertiliidae). J. Molluscan Stud. 68:365–384.

Kearse, M., R. Moir, A. Wilson, S. Stones-Havas, M. Cheung, S. Sturrock, S. Buxton, A. Cooper, S. Markowitz, C. Duran, et al. 2012. Geneious Basic: an integrated and extendable desktop software platform for the organization and analysis of sequence data. Bioinformatics 28:1647–1649.

Land, M. F., and D.-E. Nilsson. 2012. Animal eyes. Second. Oxford Univ. Press, Oxford.

Lande, R. 1978. Evolutionary mechanisms of limb loss in tetrapods. Evolution 32:73–92.

Langecker, T. G., and G. Longley. 1993. Morphological adaptations of the Texas blind catfishes *Trogloglanis pattersoni* and *Satan eurystomus* (Siluriformes: Ictaluridae) to their underground environment. Am. Soc. Icthyol. Herpetol. 1993:976–986.

Larkin, M. A., G. Blackshields, N. P. Brown, R. Chenna, P. A. McGettigan, H. McWilliam, F. Valentin, I. M. Wallace, A. Wilm, R. Lopez, et al. 2002. ClustalW and ClustalX version 2. Bioinformatics 23:2947–2948.

Leys, R., S. J. B. Cooper, U. Strecker, and H. Wilkens. 2005. Regressive evolution of an eye pigment gene in independently evolved eyeless subterranean diving beetles. Biol. Lett. 1:496–9.

Maddison, W. P., and D. R. Maddison. 2015. Mesquite: a modular system for evolutionary analysis. Version 3.04.

Malkowsky, Y., and M.-C. Götze. 2014. Impact of habitat and life trait on character evolution of pallial eyes in Pectinidae (Mollusca: bivalvia). Org. Divers. Evol. 14:173–185.

Marshall, B. A. 1999. A revision of the recent Solariellinae (Gastropoda: Trochoidea) of the New Zealand region. Nautilus 113:4–42.

McCune, A. R., and R. L. Carlson. 2004. Twenty ways to lose your bladder: common natural mutants in zebrafish and widespread convergence of swim bladder loss among teleost fishes. Evol. Dev. 6:246–259.

Miller, M. A., W. Pfeiffer, and T. Schwartz. 2010. Creating the CIPRES science gateway for inference of large phylogenetic trees. Pp. 1–8 *in* Proceedings of the Gateway Computing Environments Workshop (GCE). New Orleans.

Munk, O. 1964. The eyes of three benthic deep-sea fishes caught at great depths. Galathea Rep. 7:137–149.

Niemiller, M. L., B. M. Fitzpatrick, P. Shah, L. Schmitz, and T. J. Near. 2013. Evidence for repeated loss of selective constraint in rhodopsin of *Amblyopsid cavefishes* (Teleosti: Amblyopsidae). Evolution 67:732–748.

Niven, J. E., and S. B. Laughlin. 2008. Energy limitation as a selective pressure on the evolution of sensory systems. J. Exp. Biol. 211:1792–1804.

Ponder, W. F., and D. R. Lindberg. 1997. Towards a phylogeny of gastropod molluscs: an analysis using morphological characters. Zool. J. Linn. Soc. 119:83–265.

Poulson, T. L. 1963. Cave adaptation in amblyopsid fishes. Am. Midl. Nat. 70:257–290.

Protas, M., M. Conrad, J. B. Gross, C. Tabin, and R. Borowsky. 2007. Regressive evolution in the mexican cave tetra, *Astyanax mexicanus*. Curr. Biol. 17:452–454.

Protas, M. E., C. Hersey, D. Kochanek, Y. Zhou, H. Wilkens, W. R. Jeffery, L. I. Zon, R. Borowsky, and C. J. Tabin. 2005. Genetic analysis of cavefish reveals molecular convergence in the evolution of albinism. Nat. Genet. 38:107–111.

Protas, M. E., P. Trontelj, and N. H. Patel. 2011. Genetic basis of eye and pigment loss in the cave crustacean, *Asellus aquaticus*. Proc. Natl. Acad. Sci. USA 108:5702–5707.

Rétaux, S., and D. Casane. 2013. Evolution of eye development in the darkness of caves: adaptation, drift, or both? Evodevo 4:26.

Richardson, K. C., L. Jarret, and E. H. Finke. 1960. Embedding in epoxy resins for ultrathin sectioning in electron microscopy. Stain Technol. 35:313–323.

Ruthensteiner, B. 2008. Soft part 3D visualisation by serial sectioning and computer reconstruction. Zoosymposia 1:63–100.

Sadoglu, P. 1967. The selective value of eye and pigment loss in mexican cave fish. Evolution 21:541–549.

Sasaki, T. 1998. Comparative anatomy and phylogeny of the recent Archaeogastropoda (Mollusca: Gastropoda). Univ. Museum, Univ. Tokyo Bull. 38:1–223.

Serb, J. M., and D. J. Eernisse. 2008. Charting evolution's trajectory: using molluscan eye diversity to understand parallel and convergent evolution. Evol. Educ. Outreach 1:439–447.

Syme, A. E., and T. H. Oakley. 2012. Dispersal between shallow and abyssal seas and evolutionary loss and regain of compound eyes in cylindroleberidid ostracods: conflicting conclusions from different comparative methods. Syst. Biol. 61:314–36.

Tierney, S. M., S. J. B. Cooper, K. M. Saint, T. Bertozzi, J. Hyde, W. F. Humphreys, A. D. Austin, and S. M. Tierney. 2015. Opsin transcripts of predatory diving beetles: a comparison of surface and subterranean photic niches. R. Soc. Open Sci. 2:1–12.

Varón, A., L. S. Vinh, and W. C. Wheeler. 2010. POY version 4: phylogenetic analysis using dynamic homologies. Cladistics 26:72–85.

Vilvens, C. 2002. Description of *Zetela alphonsi* n.sp. (Gastropoda: Trochidae: Solariellinae) from Chile. Novapex 3:61–64.

Vilvens, C., and S. T. Williams. 2016. New genus and new species of Solariellidae (Gastropoda: Trochoidea) from New Caledonia, Fiji, Vanuatu, Solomon Islands, Philippines, Papua New Guinea and French Polynesia. Trop. Deep Sea Benthos. 29:267–290.

Vilvens, C., S. T. Williams, and D. G. Herbert. 2014. New genus *Arxellia* with new species of Solariellidae (Gastropoda: Trochoidea) from New Caledonia, Papua New Guinea, Philippines, Western Australia, Vanuatu and Tonga. Zootaxa 3826:255–281.

von Salvini-Plawen, L., and E. Mayr. 1977. On the evolution of photoreceptors and eyes. Evol. Biol. 10:207–263.

Warrant, E. J., S. P. Collin, and N. A. Locket. 2003. Eye design in deep-sea fishes. Pp. 303–322 *in* S. P. Collin and N. J. Marshall, eds. Sensory processing in aquatic environments. Springer, New York.

Wiens, J. J., P. T. Chippindale, and D. M. Hillis. 2003. When are phylogenetic analyses misled by convergence? A case study in Texas cave salamanders. Syst. Biol. 52:501–514.

Wilkens, H. 2001. Convergent adaptations to cave life in the *Rhamdia laticauda* catfish group (Pimelodidae, Teleostei). Environ. Biol. Fishes 62:251–261.

Wilkens, H., and U. Strecker. 2003. Convergent evolution of the cavefish *Astyanax* (Characidae, Teleostei): genetic evidence from reduced eye-size and pigmentation. Biol. J. Linn. Soc. 80:545–554.

Williams, S. T. 2012. Advances in molecular systematics of the gastropod superfamily Trochoidea. Zool. Scr. 41:571–595.

Williams, S. T., L. M. Smith, D. G. Herbert, B. A. Marshall, A. Warén, S. Kiel, P. Dyal, K. Linse, C. Vilvens, and Y. Kano. 2013. Cenozoic climate change and diversification on the continental shelf and slope: evolution of gastropod diversity in the family Solariellidae (Trochoidea). Ecol. Evol. 3:887–917.

Yamamoto, Y., D. W. Stock, and W. R. Jeffery. 2004. Hedgehog signalling controls eye degeneration in blind cavefish. Nature 431:844–887.

Zharkova, I. S. 1970. Reduction of the organs of vision in deep sea mysids. Zool. Zhurnal 49:685–693.

Associate Editor: D. Rabosky
Handling Editor: J. Conner

Supporting Information

Additional Supporting Information may be found in the online version of this article at the publisher's website:

Supplementary Data 1 as PDF: Phylogenetic reconstruction using combined MrBayes analysis of COI, 12S, 18S, and 28S fragments for all available specimens ($n = 119$).
Supplementary Data 2 as PDF: Phylogenetic reconstruction using MrBayes for COI fragments for all available specimens ($n = 201$).
Supplementary Data 3 as PDF: Phylogenetic reconstruction using MrBayes for 12S fragments for all available specimens ($n = 225$).
Supplementary Data 4 as PDF: Ancestral state reconstructions for four morphological characters of the eye.
Supplementary Data 5 as PDF: Tomographic models of eye anatomy in Solariellidae.
Supplementary Data 6 as PDF: Collection and sequence data for all specimens included in phylogenetic analyses, including those not examined for eye morphology.